

Numerical Simulation of Turbulent Flow Control at Pipe Inlet to Advance Flow Relaminarization

V. G. Lushchik^{a,*}, M. S. Makarova^{a,**}, and A. I. Reshmin^{a,***}

^aMoscow State University, Institute of Mechanics, Moscow, Russia

*e-mail: vgl_41@mail.ru

**e-mail: april27_86@mail.ru

***e-mail: alexreshmin@rambler.ru

Received July 4, 2022; revised October 25, 2022; accepted October 26, 2022

Abstract—Various methods of flow relaminarization in a pipe are considered by means of controlling the average and turbulent flow parameters. For numerical simulation of flows with turbulence growth and suppression it is proposed to use a three-parameter RANS turbulence model, which has shown good results in modeling existing experiments on relaminarization. Calculations for three variants of inlet devices with different velocity profiles and the same small-scale turbulence at the inlet show the possibility of achieving flow relaminarization in pipes at Reynolds numbers $Re > 10000$. Among three variants of inlet devices considered, the most effective one is the variant with organization of a two-zone flow with slow flow in the central region of the pipe and accelerated flow in the near-wall region. In this version, relaminarization occurs up to the Reynolds number $Re^* = 16000$. It is shown that decrease in the turbulence intensity and scale leads to an even larger value of the relaminarization Reynolds number Re^* .

Keywords: RANS-turbulence model, pipe, relaminarization, entry devices

DOI: 10.1134/S0015462822601954

As noted in [1], an increase in the energy consumption for pumping gas or liquid through pipes and, as a result, an increase in the operating costs are associated with increase in the pressure losses due to friction in the turbulent flow regime. In the case of flow relaminarization, i.e., in turbulent-to-laminar flow transition, the friction losses can be significantly reduced. For example, in flow in round pipe with the Reynolds number of the order of 25000, these losses will be reduced by an order of magnitude.

In [1] a series of the methods used for relaminarization of turbulent flow in pipes are reviewed. The methods which are associated with the mechanical motion of the walls in a certain channel cross-section [2] or the impact on the flow parameters in a certain channel cross-section and change in the flow structure or velocity profile are developed. Experimental results that demonstrate the complete relaminarization of developed turbulent flow by acting on the flow of rotors installed in the flow, which change the flow structure, as well as by injecting liquid into the flow both from the pipe walls perpendicular to the flow and along the walls are presented [3].

To suppress turbulence in pipe, special forming devices that appropriately modify the profile of the average velocity at outlet are used. In [1], structures which include partitions with holes placed in flow and special nozzles that accelerate flow in a certain area are used for flow relaminarization. Two methods of forming the velocity profile at the inlet to the relaminarization section of turbulent flow were used. The first method consisted in installing an annular insert in the central part of pipe whose inlet was covered by a perforated grid that creates hydraulic resistance. The satellite flow passed through the annular gap between the insert and the pipe. The velocity of the central flow passing through a circular insert with a grid was lower than the velocity of the satellite flow passing in the peripheral part of the pipe. The second method also consisted in organizing an axisymmetric flow in the pipe with the higher velocity near the pipe wall. To do this, air that forms the satellite flow was supplied to the area near the pipe wall at the higher velocity.

In [1], using the first method, the relaminarization of the turbulent flow was experimentally obtained at $Re = 3800$, while using the second method – at $Re = 6000$. Increase in the Reynolds number of relam-

inarization in the second flow control method can be explained by a lower level of turbulence in the central flow compared to the level of turbulence generated by the perforated grid in the first method.

Various methods of reducing the turbulence intensity have been used. In [4, 5], grids and honeycomb were used to control turbulent flow. The results obtained in these studies showed that with the help of the used grids and honeycombs, the turbulence level can be reduced by a certain amount, but flow relaminarization cannot be achieved. In studies of turbulence transition in submerged and coaxial jets [6–8] and in pipe [9], honeycombs made of polished metal pipes of 1 mm in diameter and with wall thickness of 0.05 mm and a radius-dependent length, were also used to form flows with a given input velocity profile and low-intensity and fine-scale turbulence. Modern technologies expand the possibilities of using honeycombs. In [10], the velocity profile in the flow is formed using honeycombs with a variable radius length of channels made using a 3D printer.

There are other ways to form the desired velocity profiles in jets and channels. In [11, 12], a device was used for the formation of laminar submerged jets, which makes it possible to create a smooth velocity profile with the turbulence intensity less than 1% at the Reynolds numbers above 10000 in the initial section of a jet with a diameter of 0.12 m. The low turbulence level and the required velocity profile were formed independently. To create a velocity profile, a short diffuser with a high degree of expansion and a permeable partition in the output section was used [13].

An analysis of the experimental results obtained in [1] shows that to achieve the higher Reynolds number at which relaminarization occurs, it is necessary to form a flow not only with the lower turbulence level, but also with the optimum velocity profile. This conclusion can be considered to be confirmed by authors [1] in the later work [10], where 3D-printed profiled honeycombs with small cells generating small-scale turbulence with a low intensity level were used to form the most optimal input M-shaped velocity profile. The maximum achievable Reynolds number for complete relaminarization, which was obtained at the same time, was about 10000.

Review [14] presents the results of experimental studies, in which the transition to the turbulent flow regime in pipes over a sufficiently long length at a low turbulence level at the inlet occurred at the Reynolds numbers up to $Re = 10^5$.

As for calculations of the flow relaminarization process in the studies mentioned above, they are either not available or they are not as convincing as the experimental results. In [3] the perturbation methods are developed using direct numerical simulation (DNS) of the pipe flow, and then they are implemented and tested in experiments. DNS simulates flow in the five-diameter pipe with periodic boundary conditions imposed in the axial direction. Initially, laminar flow is perturbed and the behavior of the solution is monitored at various perturbation levels to determine the level beyond which turbulence occurs. It is impossible to trace the process of relaminarization at such a small length and when periodic boundary conditions are specified. In [15], the definition of nonequilibrium turbulence was introduced. This is turbulence whose characteristics are not determined by the average velocity profile in the section under consideration. For this definition, examples of nonequilibrium turbulent flows are flows behind a grid with a constant velocity, as well as flows behind input devices, for example, honeycombs that form the velocity profile and turbulence characteristics independently.

In [15, 16], flows with inhomogeneous (trapezoidal, M-shaped and Λ -shaped) velocity profiles and small-scale turbulence at the inlet were experimentally and numerically investigated. The flow parameters were determined by input devices with variable hydraulic resistance of the honeycomb type, whose cell size is much smaller than the thickness of the layer with the velocity gradient. The peculiarity of such flows is that in them, over a considerable length, the intensity of turbulent transport processes is determined by the energy and scale of turbulence generated by the input devices that form the velocity profile. In all types of these flows, it was found that at the site of turbulence energy growth, the turbulent transport coefficients were significantly lower than at the subsequent site of developed turbulence.

To calculate the turbulent nonequilibrium flows presented in [15, 16], the RANS turbulence model was used, in which the transport equations are written for three parameters [17]: the turbulence energy $E = 0.5 \sum \langle u_i^2 \rangle$, the shear stress $\tau = -\langle u'v' \rangle$ and the parameter $\omega = E/L^2$ containing the turbulence scale L . All constants in the transport equations were determined from an analysis of three reference flows measured with high reliability: the flow behind a grid without velocity gradient, the flow behind a grid with constant velocity gradient, and developed turbulent flow in channel [17]. Numerical optimization in solving equations for turbulent flow in pipe was carried out only for three constants, and the optimization was carried out in a predetermined and rather narrow range of changes in these constants, which is associated with scattering the experimental data for flows behind the grid. When calculating flows different

from the reference ones (see, for example, in [16]), the values of the constants did not change and no empirical functions that depend on the problem parameters were introduced.

This turbulence model has been thoroughly tested over a wide class of boundary layer problems. The calculations of the flow in annular, flat and circular channels at various Reynolds numbers [18–20], boundary layer turbulence transition at a high level of external disturbances [21] in all cases showed satisfactory agreement of the results of calculations and experiments. A good coincidence was also demonstrated by the results of a comparative analysis of the viscous liquid flow in a flat channel with injection and suction through opposite walls obtained using this turbulence model and DNS [22].

Calculations of turbulent flow in a circular diffuser with a small opening angle also showed a good agreement with the results of thermoanemometric measurements of the velocity and Reynolds stress profiles [23]. In [24], calculations of the critical (threshold) Reynolds number of turbulence transition in the pipe were carried out with the help of this model at initial cross-section constant parameters. It has been shown that the critical Reynolds number depends not only on the turbulence intensity at inlet, but also on the turbulence scale. The critical Reynolds number may increase with an increase in the input turbulence intensity, if the input turbulence scale decreases at the same time. This explains the effect of relaminarization of turbulent flow after turning on the rotors placed into the pipe [3], which seemed surprising to the researchers who received it.

Confirmation of the operability and universality of the model verified in this class of problems can be considered to be the main result, since all calculations were carried out without change in the constants included in the equations for the characteristics defined in the pioneering study [17].

The aim of the present study is to calculate flows, in which the experimental data [1] on the relaminarization of turbulent flow in a pipe were obtained, using the three-parameter RANS model of sheared turbulence [17], to analyze the results obtained and to study numerically three variants of input conditions differing in the shape of the velocity profile and a low turbulence level that provide relaminarization at high Reynolds numbers.

1. METHOD FOR CALCULATING NONEQUILIBRIUM FLOW IN A PIPE

Calculation of turbulent nonequilibrium flow in pipe is carried out using the equations of continuity and motion. The problem is solved in the narrow channel approximation, where the streamwise pressure gradient is determined using the condition of constant flow rate in the pipe

$$\frac{\partial}{\partial x}(\rho u) + \frac{1}{r} \frac{\partial}{\partial r}(r \rho v) = 0, \quad \rho u \frac{\partial u}{\partial x} + \rho v \frac{\partial u}{\partial r} = -\frac{dp}{dx} + \frac{1}{r} \frac{\partial}{\partial r} \left[r \left(\eta \frac{\partial u}{\partial r} + \rho \tau \right) \right]. \quad (1.1)$$

The turbulent friction $\rho \tau = -\rho \langle u' v' \rangle$ entering into the equation of motion was determined, as in [15, 16], using the three-equation RANS turbulence model [17]

$$\begin{aligned} \rho u \frac{\partial E}{\partial x} + \rho v \frac{\partial E}{\partial r} &= -(c \rho \sqrt{EL} + c_1 \eta) \frac{E}{L^2} + \rho \tau \frac{\partial u}{\partial r} + \frac{1}{r} \frac{\partial}{\partial r} \left(r D_E \frac{\partial E}{\partial r} \right), \\ \rho u \frac{\partial \tau}{\partial x} + \rho v \frac{\partial \tau}{\partial r} &= -(3c \rho \sqrt{EL} + 9c_1 \eta) \frac{\tau}{L^2} + c_2 \rho E \frac{\partial u}{\partial r} + \frac{1}{r} \frac{\partial}{\partial r} \left(r D_\tau \frac{\partial \tau}{\partial r} \right) - D_\tau \frac{\tau}{r^2}, \\ \rho u \frac{\partial \omega}{\partial x} + \rho v \frac{\partial \omega}{\partial r} &= -(2c \rho \sqrt{EL} + 1.4c_1 \eta f_\omega) \frac{\omega}{L^2} + \left[\frac{\tau}{E} - 2c_3 \operatorname{sgn} \left(\frac{\partial u}{\partial r} \right) \right] \rho \omega \frac{\partial u}{\partial r} + \frac{1}{r} \frac{\partial}{\partial r} \left(r D_\omega \frac{\partial \omega}{\partial r} \right), \\ D_\varphi &= a_\varphi \sqrt{EL} + \alpha_\varphi \eta (\varphi = E, \tau, \omega, q_r), \quad L = \sqrt{E/\omega}, \quad f_\omega = 1 - \frac{1}{2c_1} \left(\frac{L}{E} \frac{\partial E}{\partial r} \right)^2. \end{aligned} \quad (1.2)$$

The model constants are as follows: $c = 0.3$; $c_1 = 5\pi/4$; $c_2 = 0.2$; $c_3 = 0.04$; $a_E = a_\omega = 0.06$; $a_\tau = 3a_E = 0.18$; $\alpha_E = \alpha_\tau = 1$; and $\alpha_\omega = 1.4$.

The boundary conditions on the wall, on the axis of pipe, and in the entry section are as follows:

$$\begin{aligned} u = 0, \quad v = 0, \quad E = \frac{\partial E}{\partial r} = \tau = 0 \quad (r = D/2), \\ \frac{\partial u}{\partial r} = v = 0, \quad \frac{\partial E}{\partial r} = \frac{\partial \omega}{\partial r} = \tau = 0 \quad (r = 0), \\ p = \text{const}, \quad u = u(r), \quad E = E(r), \quad L = L(r), \quad \tau = \tau(r). \end{aligned} \quad (1.3)$$

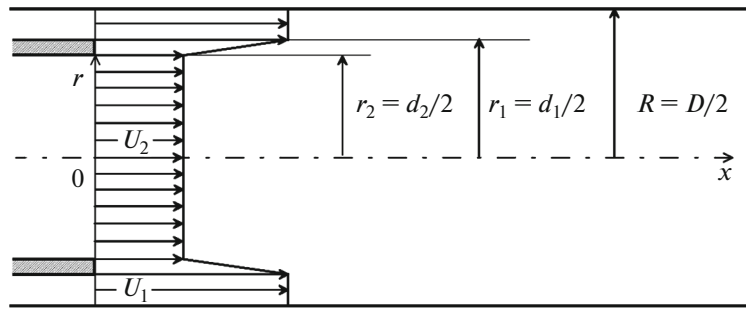


Fig 1. Scheme of calculations.

Equations (1.1)–(1.2) were solved numerically by the sweep method based on finite-spaced approximation. A computational grid was used with a non-uniform step along the pipe radius, thickening near the wall. The step along the streamwise coordinate was taken automatically depending on the given calculation accuracy.

The scheme of calculations is presented in Fig. 1. The given velocity profile at the entry into the relaminarization region was taken to correspond the profile used in the experiments [1]. In a pipe, $D = 2R = 30$ mm in inside diameter, two co-flows separated by an annular insert were organized, with $d_1 = 2r_1 = 28$ mm and $d_2 = 2r_2 = 26$ mm diameters. An annular near-wall flow “1” at the mean-flow-rate velocity U_1 issues from a 1 mm-wide gap between the annular insert and the pipe. The central flow “2” at the mean-flow-rate velocity U_2 issues from an annular insert. The co-flow velocity ratio was taken to be $U_1/U_2 = 1.67$, which corresponds to the flow rate ratio $Q_1/Q_2 \approx 0.3$.

The flow calculation (as well as the relaminarization section) starts downstream of the annular insert (see Fig. 1). The initial turbulence characteristics are not precisely known and can be specified approximately. In the central flow, the turbulence intensity is determined by the conditions of passage through grid holes with $d_3 = 3.3$ mm in diameter, downstream of which it will be sufficiently high. However, at the cylindrical insert length $L = 200$ mm ($L/d_2 \approx 7$), in the beginning of the calculation section, the turbulence intensity will decrease significantly. In the central flow, the value of the turbulence intensity $e_{02} = \sqrt{E_{02}}/U_2 = 0.05$ ($\sqrt{E_{02}}/U = 0.044$) was set as the initial conditions (subscript “0”). The initial value of the turbulence scale L_{02} in the central flow was set close to the diameter of the grid holes, so that the relative scale $l_{02} = L_{02}/R = 0.2$.

The turbulent Reynolds numbers of the central flow $Re_{t02} = \sqrt{E_{02}}L_{02}/\nu = (e_{02}/l_{02}) Re/2$ were $Re_t = 17$ at $Re = 3800$ and $Re_t = 20$ at $Re = 4500$.

When setting the initial turbulence parameters for the peripheral flow, the following was taken into account. In the 1 mm-wide gap between the annular insert and the pipe, flow is close to laminar, and the perturbations there can be considered to be minimum. However, for flow around the edge of the insert with the thickness of 1 mm, the flow turbulence occurs with a scale approximately equal to the edge thickness. For peripheral flow the following initial values of intensity $e_{01} = \sqrt{E_{01}}/U_1 = 0.007$ ($\sqrt{E_{01}}/U = 0.01$) and turbulence scale $l_{01} = L_{01}/R = 0.07$ were taken in the calculations.

The entry shear stress in both flows was taken to be $\tau = -\beta\sqrt{EL}(\partial u/\partial r)$ in accordance with the Prandtl formula where $\beta = 0.23$ [16]. The velocity profile at the entry in the peripheral and central zone were taken to be homogeneous and varied linearly at the annular insert edge (Fig. 1).

The calculations were carried out at the Reynolds numbers $Re = DU/\nu$ presented in [1]. Here, D , U , ν are the pipe diameter, the mean-flow-rate velocity, and the kinematic air viscosity.

The results of the numerical investigation for the Reynolds numbers $Re = 3800$ and 4500 in the case of the first relaminarization mode [1] are presented in Figs. 2–7.

At the Reynolds number $Re = 3800$, as in experiment [1], relaminarization is reached on the length $z = x/D = 100$, which is confirmed by the value $u_{cl}/U = 1.8$ close to the value $u_{cl}/U = 2$ for the laminar flow regime (Fig. 2). In this case, the turbulence intensity on the pipe axis $e_{cl} = \sqrt{E_{cl}}/U$ (Fig. 3a) tends to zero and the drag coefficient $\xi = (8\rho U^2)(\rho\nu\partial u/\partial r)_w$ (Fig. 3b) approaches the value $\xi = 64/Re$ in the lam-

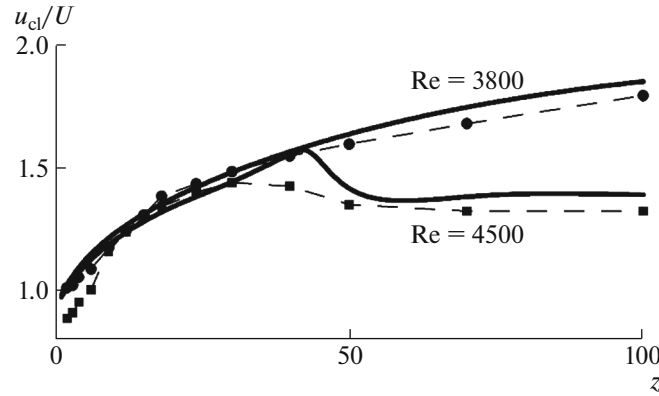


Fig. 2. Variation in the dimensionless flow velocity at the pipe axis u_{cl}/U along the relaminarization region length $z = x/D$ for two Reynolds numbers $Re = 3800$ and 4500 ; points relate to experiment [1] and curves to the calculations.

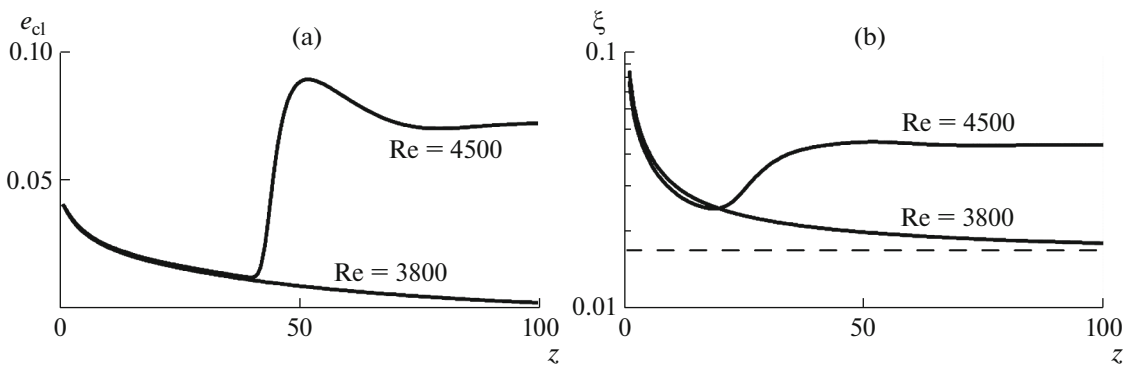


Fig. 3. Calculated variation in the turbulence intensity on the pipe axis $e_{cl} = \sqrt{E_{cl}}/U$ (a) and the resistance coefficient ξ (b) along the pipe length $z = x/D$ for two Reynolds numbers $Re = 3800$ and 4500 ; the dashed line $\xi = 64/Re$ corresponds to the laminar flow regime at $Re = 3800$.

inar flow regime. At the Reynolds number $Re = 4500$ under the same entry conditions relaminarization was not obtained, as in experiment [1] (see Figs. 2 and 3).

It should be mentioned that the term “achievement of relaminarization” used in the paper implies the tendency of the relative velocity u_{cl}/U and turbulence intensity e_{cl}/U on the pipe axis to the values $u_{cl}/U \rightarrow 2$ and $e_{cl}/U \rightarrow 0$, respectively, and the tendency of the drag coefficient ξ to value $\xi \rightarrow 64/Re$.

Figure 4 shows that the velocity profile u/U at $z = 100$ is close to the Poiseuille profile in the case of flow relaminarization ($Re = 3800$) and to the velocity profile for developed turbulent flow in the case when relaminarization does not occur ($Re = 4500$).

As can be seen in Fig. 5, in the case of flow relaminarization ($Re = 3800$) the sharp decline of the turbulence intensity $e = \sqrt{E}/U$ is observed in the region near the pipe wall as in experiment [1]. According to [1], this means the suppression of turbulence generation in the wall region, where it reaches maximum in the absence of relaminarization.

In Fig. 6 the calculated variation in the maximum turbulence generation $P_m = -(\rho\tau \partial u/\partial r)_m$ (Fig. 6a) and its coordinate r_m/R (Fig. 6b) along the length $z = x/D$ is presented for the Reynolds numbers that correspond to achievement and absence of relaminarization. The results obtained indicate that in the case of flow relaminarization ($Re = 3800$) the turbulence generation is suppressed and its maximum is displaced from the pipe wall toward the axis. If relaminarization is not achieved ($Re=4500$), the turbulence generation maximum increases, as the developed turbulent flow regime is achieved at $z = 100$ and the generation maximum location r_m/R remains in the wall region. The results obtained show that the relaminarization mechanism is based on the weakening of near-wall turbulence generation.

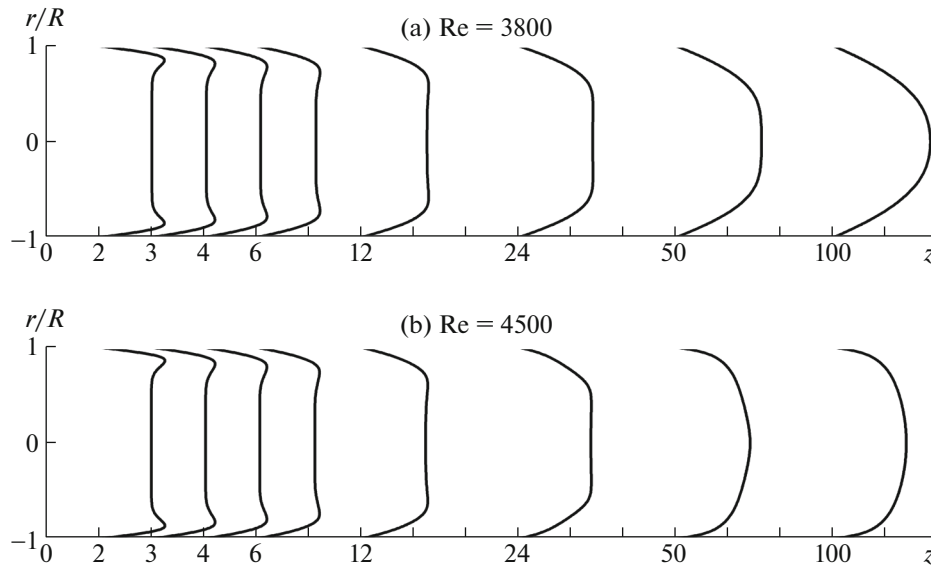


Fig. 4. Calculated velocity profiles u/U at the Reynolds numbers $Re = 3800$ (a) and 4500 (b) in the cross-sections $z = 2, 3, 4, 6, 12, 24, 50,$ and 100 along the pipe length.

The calculation results presented in Figs. 2–6 only qualitatively correspond to the experimental data [1] which can be explained by the deficient information on the turbulence characteristics at the entry. Nevertheless, the results obtained confirm the possibility of flow relaminarization with decelerated flow in the central region of pipe and accelerated flow in the wall region. The given Reynolds number $Re = 3800$, at which relaminarization occurs, corresponds to the one obtained in the experiment [1] at the input values of the turbulence scale and intensity, the estimation of them in the calculation was carried out approximately, in the absence of experimental data.

This fairly low value of the relaminarization Reynolds number can be attributed to a fairly high turbulence intensity in the central region due the presence of the turbulizing grid organizing a decelerated flow in the central part of the pipe.

The fact that the possibility of relaminarization considerably depends on the entry conditions was noted in [1]. For example, when varying the hole diameter in the grid of the annular insert from $d_3 = 3.3$ mm to $d_3 \leq 2.8$ mm or $d_3 \geq 4$ mm, relaminarization was not achieved at the Reynolds number $Re = 3800$. With variation in the mesh hole diameter, its porosity changes and, therefore, the co-flow velocity ratio U_1/U_2 increases with decrease in d_3 and decreases with increase in d_3 . The turbulence intensity $e_{02} = \sqrt{E_{02}}/U$ and scale L_{02}/R at the entry into the central zone also vary.

The numerical investigation was performed for two flow versions qualitatively corresponding to the above-mentioned experiments with reduced and augmented hole diameters of the mesh of the annular insert. In the first version $U_1/U_2 = 2.3$, $e_{02} = \sqrt{E_{02}}/U = 0.045$, and $L_{02}/R = 0.18$, while in the second version $U_1/U_2 = 1.2$, $e_{02} = \sqrt{E_{02}}/U = 0.07$, and $L_{02}/R = 0.3$. In both versions, the turbulence characteristics at the entry into the near-wall flow remained unchanged. In both calculated cases relaminarization was not achieved at the Reynolds number $Re = 3800$.

Decrease in the turbulence intensity at the entry into the central region in the absence of the turbulizing mesh made it possible to increase the relaminarization Reynolds number for the second mode of flow organization used in [1] to $Re = 6000$.

The numerical investigation was performed for two Reynolds numbers, $Re = 6000$ and $Re = 7000$ under the following entry conditions: $U_1/U_2 = 1.67$, $e_{02} = \sqrt{E_{02}}/U = 0.01$, $l_{02} = L_{02}/R = 0.2$, $e_{01} = \sqrt{E_{01}}/U = 0.01$, $l_{01} = L_{01}/R = 0.1$. The turbulent Reynolds number for the central flow were $Re_t = 6$ for $Re = 6000$ and $Re_t = 7$ for $Re = 7000$.

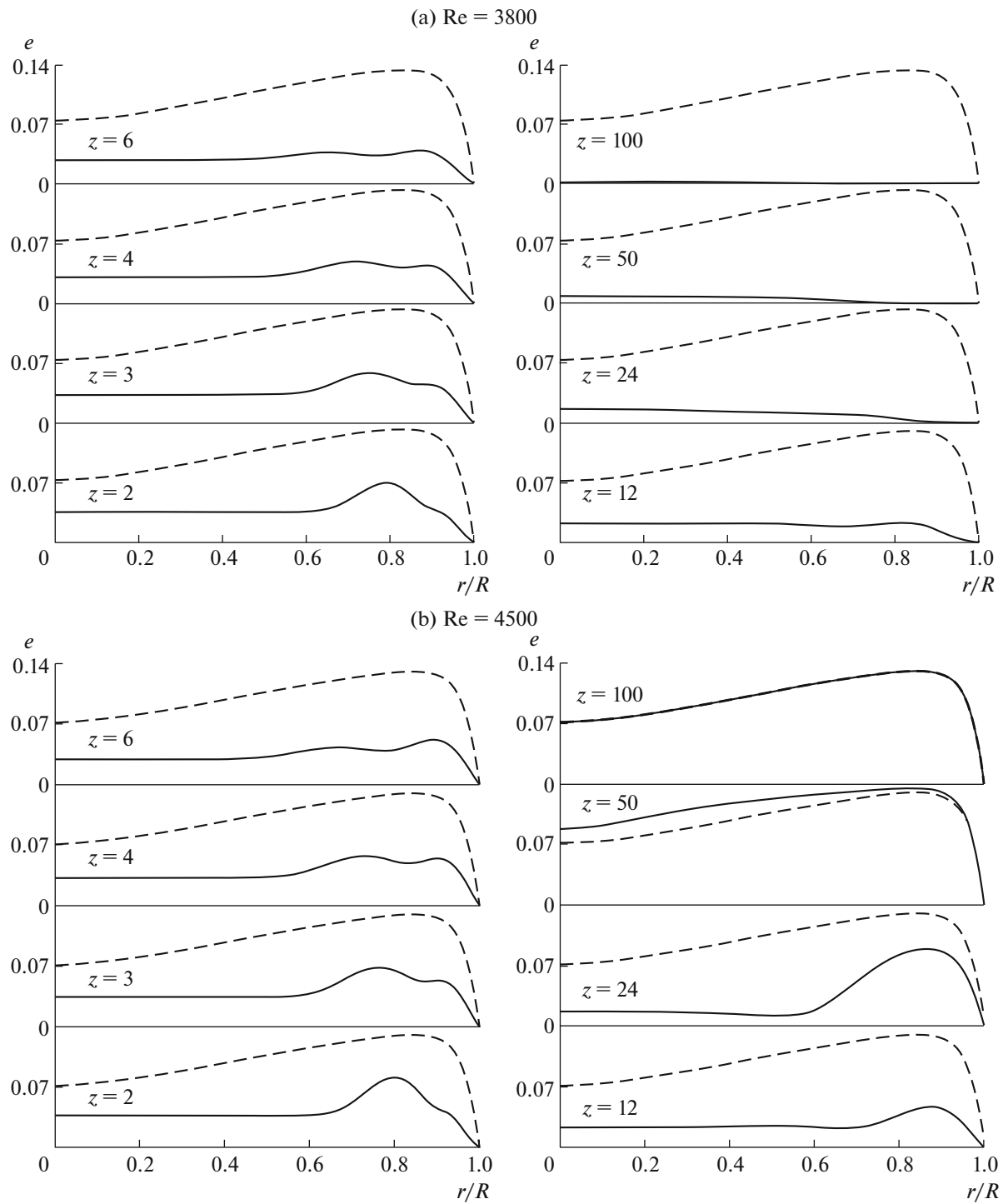


Fig. 5. Calculated turbulence intensity profiles $e = \sqrt{E}/U$ at the Reynolds numbers $Re = 3800$ (a) and 4500 (b) in the cross-sections $z = 2, 3, 4, 6, 12, 24, 50,$ and 100 along the pipe length. Dashed curves correspond to the uncontrolled turbulent flow for reference.

We note that, as relaminarization is reached with increase in the Reynolds number from $Re = 3800$ to 6000 , the turbulent Reynolds number Re_t decreases from 20 to 7 .

In Fig. 7 variation in the dimensionless flow velocity u_{cl}/U (a) and the turbulence intensity $e_{cl} = \sqrt{E_{cl}}/U$ (b) at the pipe axis along the relaminarization region length $z = x/D$ is presented. In calculations flow relaminarization was achieved only at $Re = 6000$.

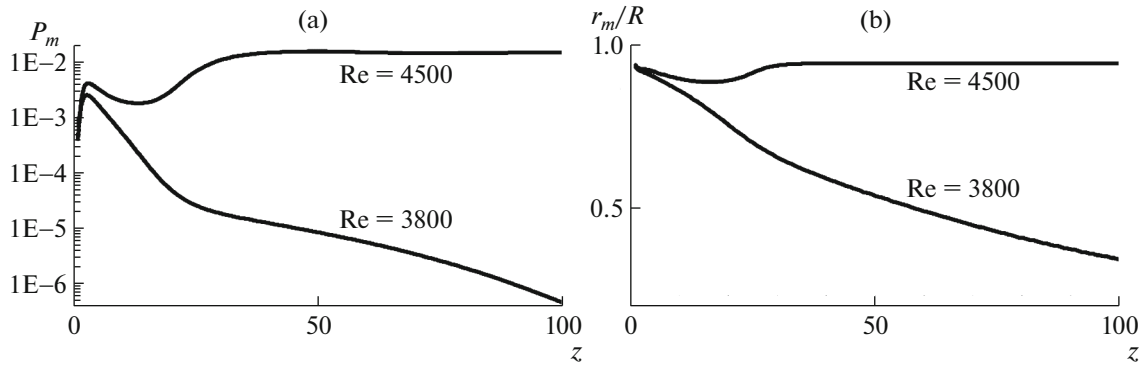


Fig. 6. Calculated variation in the maximum turbulence generation $P_m = -(\rho\tau \partial u / \partial r)_m$ (a) and the coordinate of generation maximum r_m/R (b) along the length $z = x/D$ at two Reynolds numbers $Re = 3800$ and 4500 .

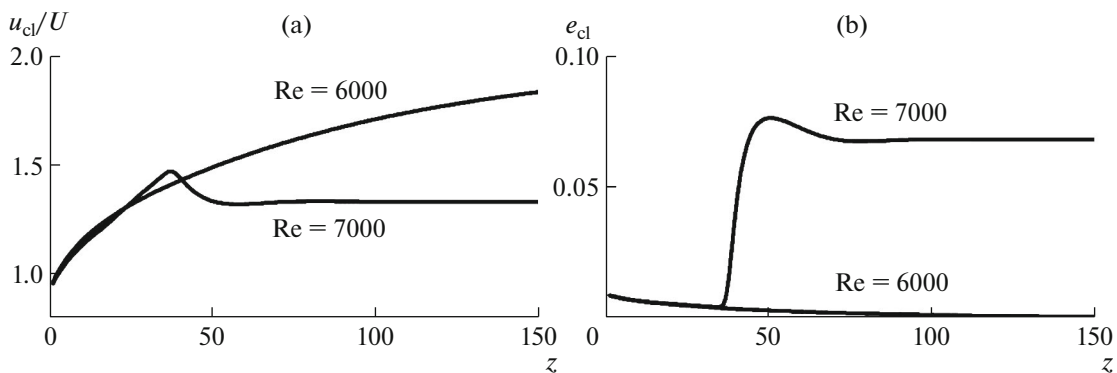


Fig. 7. Calculated variation in the dimensionless flow velocity u_{cl}/U (a) and the turbulence intensity $e_{cl} = \sqrt{E_{cl}}/U$ (b) on the pipe axis along the relaminarization region length $z = x/D$ at two Reynolds numbers $Re = 6000$ and 7000 .

2. EFFECT OF VELOCITY PROFILE SHAPE ON RELAMINARIZATION ACHIEVEMENT AT A LOW LEVEL OF ENTRY DISTURBANCES

An analysis of the experimental results obtained in [1] allows one to conclude that to increase relaminarization Reynolds number it is necessary not only reduce the entry turbulence level but also form the flow at the entry with the optimal velocity profile. In this connection, it is of interest to investigate the effect of the entry velocity profile on the possibility of flow relaminarization at a low intensity level of the turbulence at the entry.

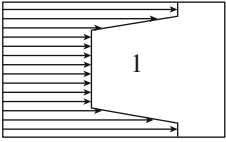
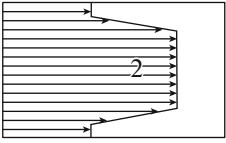
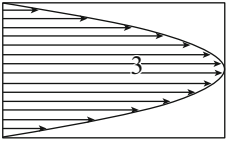
The flow organization with a given velocity profile was demonstrated in [9] using contoured honeycombs made of thin-wall pipes of small diameter generating low-intensity and small scale of the order of the honeycomb pipe diameter.

Numerical investigation was carried out for three versions of entry velocity profiles, its form is presented in the Table 1:

- version 1 with an M-shaped velocity profile analogous to that considered in [1, 15, 16] with the parameters $r_1/R = 0.9$, $r_2/R = 0.87$, and $U_1/U_2 = 1.5$;
- version 2 with the Λ -shaped velocity profile analogous to that considered in studies [15, 16] with the parameters $r_1/R = 0.9$, $r_2/R = 0.87$, and $U_1/U_2 = 0.6$;
- version 3 with a parabolic velocity profile considered in study [9].

In all the three versions the turbulence characteristics at the entry were the same and were taken to be as follows: the turbulence intensity based on the local velocity u , $e_0 = \sqrt{E_0}/u = 0.01$ and the turbulence scale $L_0/R = 0.05$.

Table 1

Version of entry device	Reynolds number		Notation same as in Figs. 19 and 13
	Re_1^*	16000	1*
	Re_1	17000	1
	Re_2^*	12000	2*
	Re_2	13000	2
	Re_3^*	10000	3*
	Re_3	11000	3

The parabolic velocity profile (version 3) realized in [9] using a honeycomb is interesting to the fact that under relaminarization the velocity profile will tend to its original shape. The calculation showed the drag coefficient ξ for this version will be less on the whole length then for other versions of initial profiles under consideration and will be close to the laminar value $\xi = 64/Re$.

As in [1], the attainment of the relaminarization regime in the calculations was determined from variation in the dimensionless velocity u_{cl}/U (Fig. 8a) and the turbulence intensity $e_{cl} = \sqrt{E_{cl}}/U$ (Fig. 8b) on the pipe axis along the pipe length and the drag coefficient ξ (Fig. 8c). The calculations performed with the step in the Reynolds number $\Delta Re = 1000$.

Figure 8 shows that relaminarization occurs in the Reynolds number ranges $Re = (16-17) \times 10^3$ for the entry device version 1, $Re = (12-13) \times 10^3$ for version 2, and $Re = (10-11) \times 10^3$ for version 3.

Variation in the relative flow velocity u_{cl}/U (a) and the turbulence intensity $e_{cl} = \sqrt{E_{cl}}/U$ (b) on the pipe axis along the relaminarization region length $z = x/D$ for the three versions of entry devices is presented in Fig. 9 at the Reynolds numbers given in Table 1.

As for the calculations at high Reynolds numbers (see Fig. 9), such calculations were also carried out for the lengths greater than 100 pipe diameters. Figure 9 shows the flow parameters in the region of flow turbulization, which occurs at $z \approx 50$. At $z > 80$, the parameters practically do not change under turbulization.

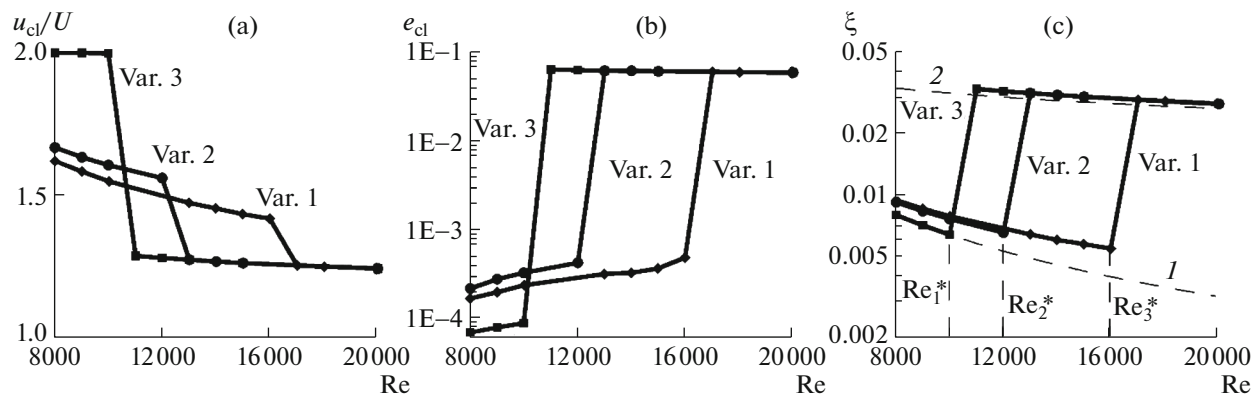


Fig. 8. Velocity u_{cl}/U (a) and turbulence intensity $e_{cl} = \sqrt{E_{cl}}/U$ (b) on the pipe axis and the resistance coefficient ξ (c) as functions of the Reynolds number $Re = DU/\nu$ for three versions of entry devices (curves and dots). Curve 1 corresponds to $\xi = 64/Re$ and curve 2 to $\xi = 0.316/Re^{1/4}$.

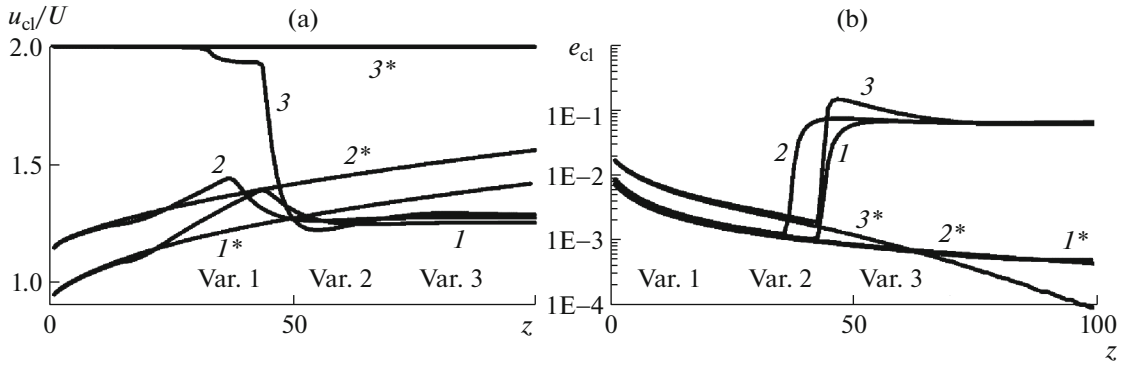


Fig. 9. Variation in the dimensionless flow velocity u_{cl}/U (a) and the turbulence intensity $e_{cl} = \sqrt{E_{cl}}/U$ (b) on the pipe axis along the relaminarization region length $z = x/D$ for three versions of entry devices.

zation. In the case of relaminarization, at $z > 100$, the flow parameters change monotonically. The flow velocity profile tends to the parabolic one, and the turbulence energy tends to zero.

To illustrate the effect of the entry velocity profile under consideration on the turbulence development the velocity profiles and turbulent characteristics were calculated for several cross-sections along the pipe length at the Reynolds number $Re = 14000$. Figure 10 shows the relative velocity $\bar{u} = u/U$, Fig. 11—the turbulence intensity $e = \sqrt{E}/U$, and Fig. 12—the shear stress $\bar{\tau} = \tau/U^2$.

At $z \leq 12$ the velocity profiles are similar to the entry profiles and their considerable restructuring begins from $z \approx 24$ and ends at $z \geq 50$ (see Fig. 10). For the entry device versions 2 and 3 the velocity profiles are similar to that in developed turbulent flow at the Reynolds number $Re = 14000$, while for version 1 the velocity profile tends to the parabolic profile and reaches it at $z > 100$.

Variation in the turbulence intensity profiles $e = \sqrt{E}/U$ (Fig. 11) is more considerable than that of the velocity profiles, particularly for $z \geq 12$. For version 1 the quantity e considerably diminishes at $z \geq 12$ and becomes near-zero at $z \geq 50$. For versions 2 and 3 the quantity e considerably increases throughout the entire pipe cross-section at $z \approx 24$, while at $z \geq 50$ it is similar in value to e for developed turbulent flow.

Of interest is the variation in the shear stress $\tau = -\langle u'v' \rangle$ obtained in the calculations; along with the derivative of the longitudinal velocity $\partial u/\partial r$, it enters into the definition of the turbulence energy generation $P = -(\rho\tau \partial u/\partial r)$.

In Fig. 12 the profiles of the dimensionless shear stress $\bar{\tau} = \tau/U^2$ in certain cross-sections along the pipe length for the three versions of initial velocity profiles are presented. For the entry device with the M-shaped entry velocity profile (version 1) having a velocity peak in the wall region $\bar{\tau}$ is positive at $z < 12$, as distinct from negative $\bar{\tau}$ values for the other two versions of initial velocities. At $z \geq 12$ $\bar{\tau}$ is near-zero, whereas for versions 2 and 3 at $z \approx 24$ it increases considerably (in absolute value) throughout the entire pipe cross-section and at $z \geq 50$ is close to the value of $\bar{\tau}$ for developed turbulent flow.

The calculated profiles of the turbulence generation $P = -(\rho\tau \partial u/\partial r)$ in certain pipe cross-sections along the pipe length for the three versions of inlet velocity profiles under consideration showed that for versions 1 and 2 the turbulence generation is maximum in the wall region, where velocity gradients are large. At $z \geq 12$ the turbulence generation is near-zero for version 1, whereas for versions 2 and 3 it increases considerably at $z \approx 24$ and is close to the value for the developed turbulent flow with a near-wall maximum at $z \geq 50$. We note that the evolution of the turbulence generation corresponds to the nature of the variation of the turbulence intensity profile (Fig. 11).

The calculated variation of the maximum value of the turbulence generation $P_m = -(\rho\tau \partial u/\partial r)_m$ and the coordinate of the generation maximum r_m/R along the pipe length is presented in Fig. 13. As in the case of experiment [1] (see Fig. 6), the results obtained indicate that in the case of relaminarization the turbulence generation is suppressed and its maximum is displaced from the pipe wall to the axis. In the absence of relaminarization a maximum of the turbulence generation increases, as the regime of developed turbulent flow is approached, and the generation maximum r_m/R remains located in the wall region.

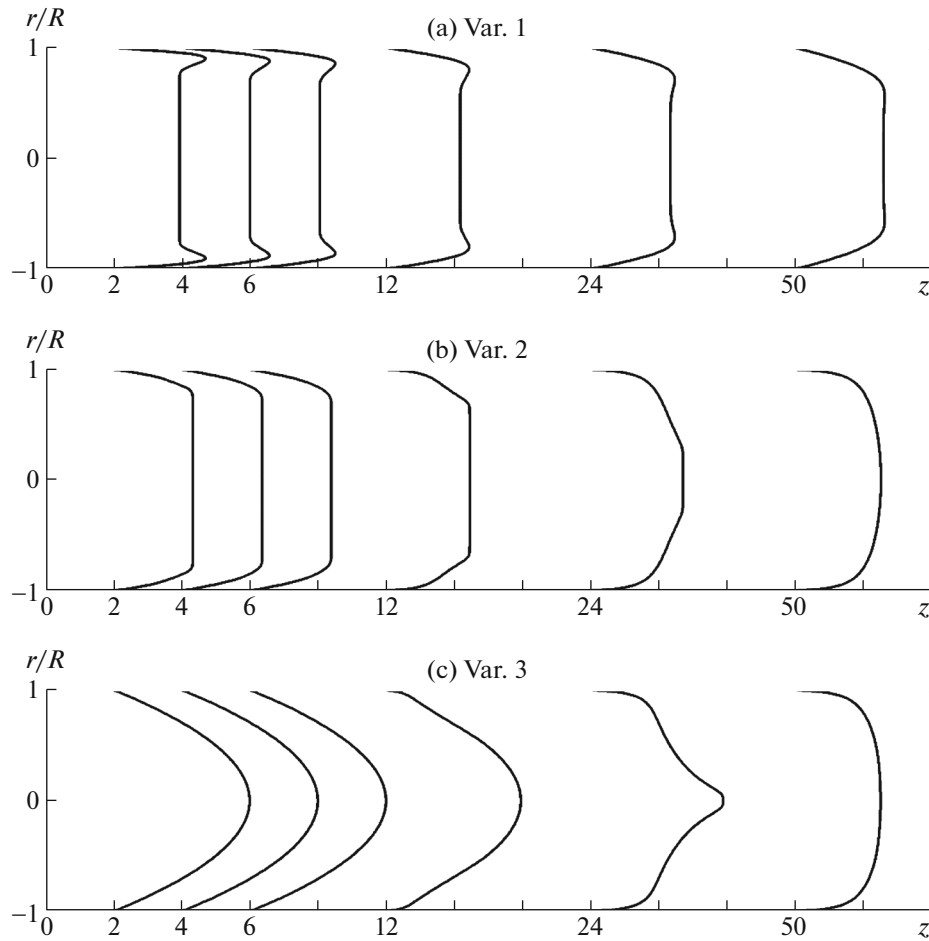


Fig. 10. Velocity profiles u/U in the cross-sections $z = 2, 4, 6, 12, 24,$ and 50 along the pipe axis at the Reynolds number $Re = 14000$ for three versions of entry devices: var. 1 (a), var. 2 (b), and var. 3 (c).

In the three versions the turbulence characteristics at the entry were identical ($e_0 = \sqrt{E_0}/u = 0.01$ and $l_{02} = L_0/R = 0.05$). For versions 1 and 2 with two-zoned flow organization at the entry section the effect of entry values of the turbulence intensity $e_{02} = \sqrt{E_{02}}/U_2$ ($l_{02} = L_{02}/R = 0.05$) and the turbulence scale $l_{02} = L_{02}/R$ ($e_{02} = \sqrt{E_{02}}/U_2 = 0.01$) was studied in the central flow on the flow relaminarization Reynolds number. These results are presented at Fig. 14.

Decrease in the turbulence intensity e_{02} in the near-wall flow considerably increases the relaminarization Reynolds number Re^* (see Fig. 14a). This increase is to a greater degree pertinent to version 1 with enlarged flow velocity near the wall than for the version 2. The effect of the entry turbulence scale l_{02} on Re^* is essential for small scales $l_{02} < 0.2$ and for $l_{02} > 0.2$ the entry turbulence scale has almost no effect on Re^* value (Fig. 14b). This indicates the sensitivity of the results of calculations to the entry value of the characteristic scale length.

SUMMARY

Using the three-parameter RANS turbulence model, the numerical study of the turbulent flow development in the round pipe at the various input parameters was carried out to determine the possibility of degeneration of flow turbulence and achievement of relaminarization of flow in the round pipe.

For given values of the turbulence scale and intensity the estimation of which in calculations carried out approximately, in the absence of experimental data, a satisfactory agreement was obtained between the flow calculation results with slow flow in the central and accelerated flows in the pipe near-wall region,

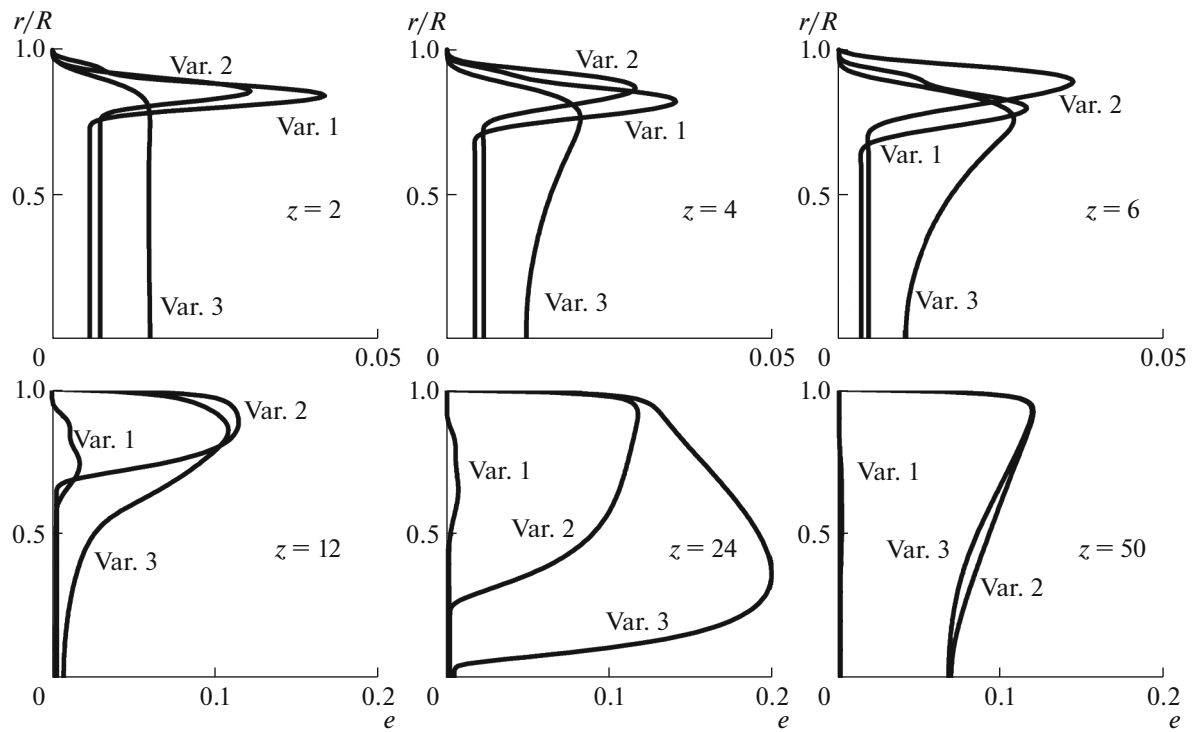


Fig. 11. Turbulence intensity profiles $e = \sqrt{E}/U$ in the cross-sections $z = 2, 4, 6, 12, 24,$ and 50 along the pipe axis at the Reynolds number $Re = 14000$ for three versions of entry devices.

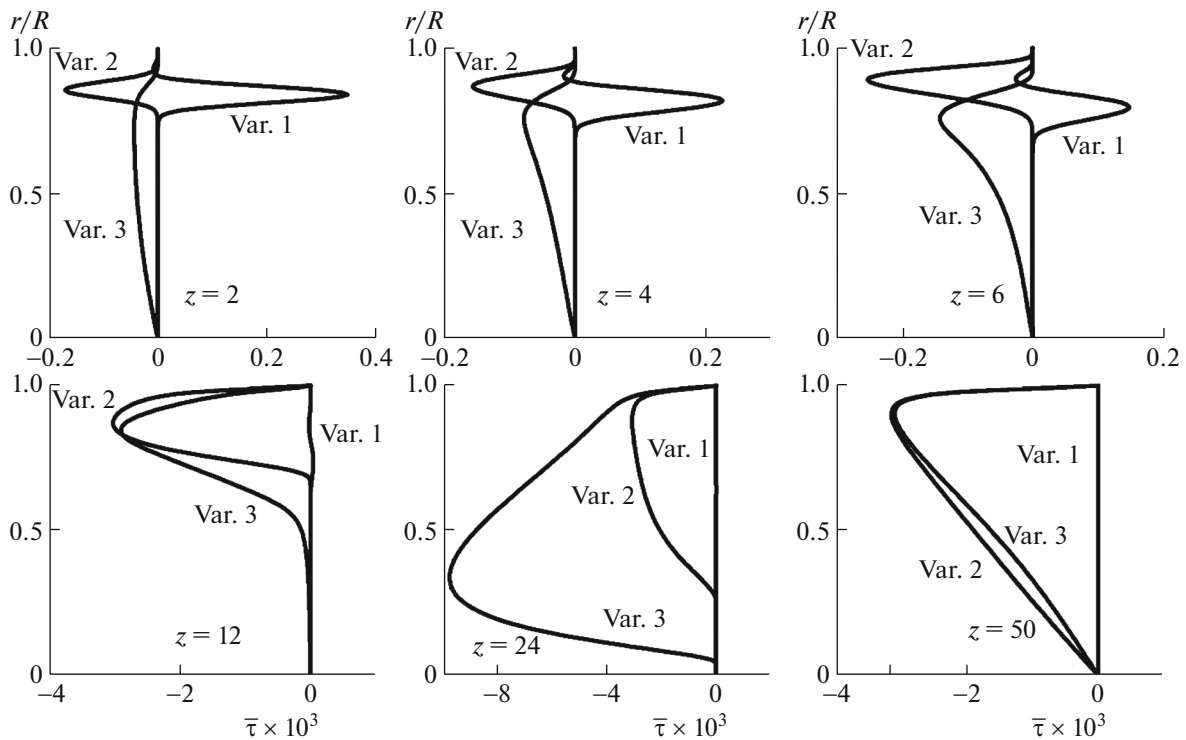


Fig. 12. Shear stress profiles $\bar{\tau} = \tau/U^2$ in the cross-sections $z = 2, 4, 6, 12, 24,$ and 50 along the pipe axis at the Reynolds number $Re = 14000$ for three versions of entry devices.

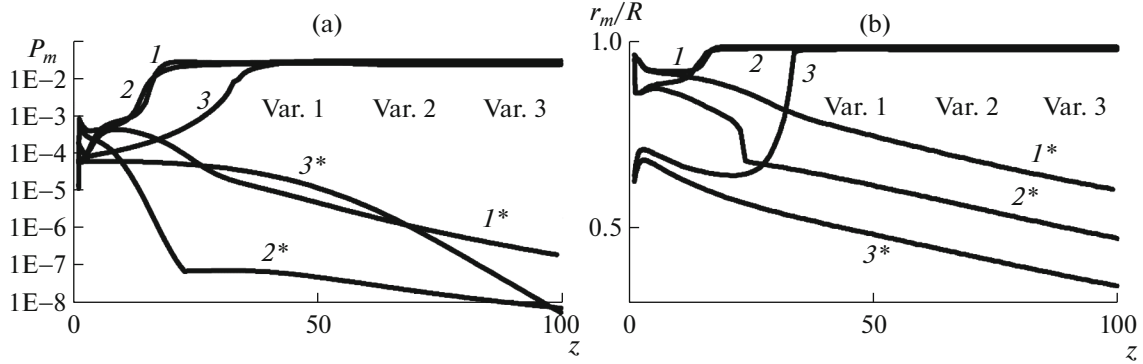


Fig. 13. Variation in the maximum turbulence generation $P_m = -(\rho\tau \partial u/\partial r)_m$ (a) and the coordinate of the maximum generation r_m/R (b) along the length $z = x/D$ for three versions of entry devices.

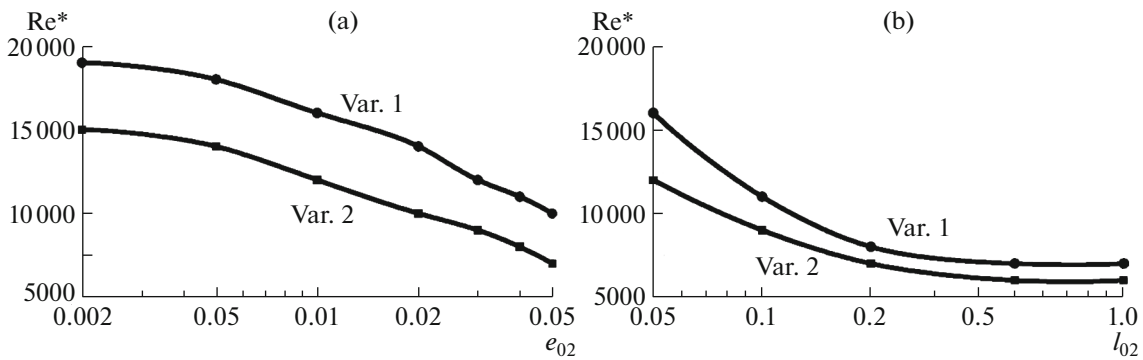


Fig. 14. Relaminarization Reynolds number Re^* as a function of the turbulence intensity $e_{02} = \sqrt{E_{02}}/U_2$ ($e_{01} = 0.01$, $l_{01} = l_{02} = 0.05$) (a) and the dimensionless turbulence scale $l_{02} = L_{02}/R$ ($l_{01} = 0.005$, $e_{01} = e_{02} = 0.01$) (b) in the central flow for two versions of entry devices (curves and points).

formed using special entry devices [1], with the experimental results on the main flow parameters and relaminarization Reynolds numbers.

The numerical study of three variants of nonhomogeneous inlet velocity profiles and a small-scale turbulence at the entry with an intensity determined from the local velocity u , $e_0 = \sqrt{E_0}/u = 0.01$ and a scale $L_0/R = 0.05$ was carried out. Calculations showed that flow relaminarization can be achieved at the Reynolds numbers more than 10000.

Three variants of flows with nonhomogeneous inlet velocity profiles are studied. The highest Reynolds number of relaminarization was obtained in variant 1, experimentally studied in [1]. In this variant, the inlet flow is slowed down in the central region and accelerated in the near-wall region of the pipe. The achieved relaminarization Reynolds number is equal to $Re^* = 16000$. For variant 2, where the accelerated flow is in the central region, and slow flow is in the near-wall region of the pipe, the relaminarization Reynolds number turned out to be less than $Re^* = 12000$. For variant 3 with the inlet parabolic velocity profile, the relaminarization Reynolds number turned out to be the smallest: $Re^* = 10000$.

It was shown that for further increase in the Reynolds number of relaminarization it is necessary to decrease the intensity and scale of turbulence at the inlet. So, for variant 1 of the forming device, reducing the input turbulence intensity from $e_0 = 1\%$ to 0.5% with the turbulence scale $l_0 = 0.05$ increases the value of Re^* from 16000 to 18000.

The obtained results of numerical study showed that the independent control of the velocity profile and turbulence characteristics in the initial section makes it possible to find an effective solution to practical and research problems, including those related to flow relaminarization in pipes. To implement such con-

trol, it is necessary to develop fairly simple and technologically advanced methods for forming flows with an optimal velocity profile and low-intensity small-scale turbulence.

FUNDING

This work is supported by the Russian Science Foundation under grant no. 20-19-00404.

OPEN ACCESS

This article is licensed under a Creative Commons Attribution 4.0 International License, which permits use, sharing, adaptation, distribution and reproduction in any medium or format, as long as you give appropriate credit to the original author(s) and the source, provide a link to the Creative Commons license, and indicate if changes were made. The images or other third party material in this article are included in the article's Creative Commons license, unless indicated otherwise in a credit line to the material. If material is not included in the article's Creative Commons license and your intended use is not permitted by statutory regulation or exceeds the permitted use, you will need to obtain permission directly from the copyright holder. To view a copy of this license, visit <http://creativecommons.org/licenses/by/4.0/>.

REFERENCES

1. Kühnen, J., Scarselli, D., Schaner, M., and Hof, B., Relaminarization by steady modification of the streamwise velocity profile in a pipe, *Flow, Turbul., Combust.*, 2018, vol. 100, pp. 919–943.
<https://doi.org/10.1007/s10494-018-9896-4>
2. Scarselli, D., Kühnen, J., and Hof, B., Relaminarising pipe flow by wall movement, *J. Fluid Mech.*, 2019, vol. 867, pp. 934–948.
<https://doi.org/10.1017/jfm.2019.191>
3. Kühnen, J., Song, B., Scarselli, D., Budanur, N.B., Riedl, M., Willis, A.P., Avila, M., and Hof, B., Destabilizing turbulence in pipe flow, *Nat. Phys.*, 2018, vol. 14, pp. 386–390.
<https://doi.org/10.1038/s41567-017-0018-3>
4. Laws, E.M. and Livesey, J.L., Flow through screens. *Annu. Rev. Fluid Mech.*, 1978, vol. 10, pp. 247–266.
<https://doi.org/10.1146/annurev.fl.10.010178.001335>
5. Lumley, J.L. and McMahon, J.F., Reducing water tunnel turbulence by means of a honeycomb, *J. Basic Eng.*, 1967, vol. 89, pp. 764–770.
<https://doi.org/10.1115/1.3609700>
6. Navoznov, O.I. and Pavel'ev, A.A., Transition to turbulence in coflowing jets, *Fluid Dyn.*, 1969, vol. 4, pp. 84–88.
<https://doi.org/10.1007/BF01032481>
7. Navoznov, O.I., Pavel'ev, A.A., and Yatsenko, A. V., The transition to turbulence in submerged jets and wakes, *Fluid Dyn.*, 1972, vol. 7, pp. 672–678.
<https://doi.org/10.1007/BF01205209>
8. Navoznov, O.I. and Pavel'ev, A.A., Influence of the initial conditions on axisymmetric jets in a parallel flow, *Fluid Dyn.*, 1980, vol. 15, pp. 488–493.
<https://doi.org/10.1007/BF01089604>
9. Kolyada, V. V. and Pavel'ev, A.A., Effect of the velocity profile at the inlet to a circular pipe on the transition to turbulence, *Fluid Dyn.*, 1986, vol. 21, pp. 650–653.
<https://doi.org/10.1007/BF01057154>
10. Kühnen, J., Scarselli, D., and Hof, B., Relaminarization of pipe flow by means of 3D-printed shaped honeycombs. *J. Fluids Eng.*, 2019, vol. 141, no. 11, p. 111105.
<https://doi.org/10.1115/1.4043494>
11. Zaiko, Y.S., Reshmin, A.I., Teplovodskii, S.K., and Chicherina, A.D., Investigation of submerged jets with an extended initial laminar region. *Fluid Dyn.*, 2018, vol. 53, pp. 95–104.
<https://doi.org/10.1134/S0015462818010184>
12. Zayko, J., Teplovodskii, S., Chicherina, A., Vedenev, V., and Reshmin, A., Formation of free round jets with long laminar regions at large Reynolds numbers, *Phys. Fluids*, 2018, vol. 30, no. 4, p. 043603.
<https://doi.org/10.1063/1.5021017>
13. Reshmin, A.I., Teplovodskii, S.K., and Trifonov, V. V., Short round diffuser with a high area ratio and a permeable partition. *Fluid Dyn.*, 2012, vol. 47, pp. 583–589.
<https://doi.org/10.1134/S0015462812050043>
14. Eckhardt B. Turbulence transition in pipe flow: 125th anniversary of the publication of Reynolds' paper. *Phil. Trans. R. Soc. A*, 2009, vol. 367, pp. 449–455.

15. Lushchik, V.G., Pavel'ev, A.A., and Yakubenko, A.E., Turbulent boundary layer control: experimental data and theoretical models. Mechanical engineering and applied mechanics. 2 (Fluid mech.), 1987, pp. 61–82.
16. Lushchik, V.G., Pavel'ev, A.A., and Yakubenko, A.E., Turbulent flows. Models and numerical investigations. A review, *Fluid Dyn.* 1994, vol. 29, pp. 440–457.
<https://doi.org/10.1007/BF02319065>
17. Lushchik, V.G., Pavel'ev, A.A., and Yakubenko, A.E., Three-parameter model of shear turbulence, *Fluid Dyn.*, 1978, vol. 13, pp. 350–360.
<https://doi.org/10.1007/BF01050525>
18. Leont'ev, A.I., Lushchik, V.G., and Makarova, M.S., Numerical investigation of tube flow with suction through permeable walls, *Fluid Dyn.*, 2014, vol. 49, pp. 362–368.
<https://doi.org/10.1134/S0015462814030077>
19. Lushchik, V.G., Makarova, M.S., and Reshmin, A.I., Laminarization of flow with heat transfer in a plane channel with a confuser, *Fluid Dyn.*, 2019, vol. 54, pp. 67–76.
<https://doi.org/10.1134/S0015462819010099>
20. Makarova, M.S. and Lushchik, V.G., Numerical simulation of turbulent flow and heat transfer in tube under injection of gas through permeable walls, *J. Phys. Conf. Ser.*, 2017, vol. 891, 012066.
<https://doi.org/10.1088/1742-6596/891/1/012066>
21. Lioznov, G.L., Lushchik, V.G., Makarova, M.S., and Yakubenko, A.E., Freestream turbulence effect on flow and heat transfer in the flat-plate boundary layer, *Fluid Dyn.*, 2012, vol. 47, pp. 590–592.
<https://doi.org/10.1134/S0015462812050055>
22. Nikitin, N.V. and Pavel'ev, A.A., Turbulent flow in a channel with permeable walls. Direct numerical simulation and results of three-parameter model, *Fluid Dyn.*, 1998, vol. 33, pp. 826–832.
<https://doi.org/10.1007/BF02698650>
23. Reshmin, A.I., Trifonov, V.V., and Teplovodskii, S.K., Turbulent Flow in a Conical Diffuser With a Small Divergence Angle at Reynolds Numbers Less Than 2000, in: Volume 1C, Symposia: *Fundamental Issues and Perspectives in Fluid Mechanics; Industrial and Environmental Applications of Fluid Mechanics; Issues and Perspectives in Automotive Flows; Gas-Solid Flows: Dedicated to the Memory of Professor Clayton T. Crowe*; 2014, American Society of Mechanical Engineers.
<https://doi.org/10.1115/FEDSM2014-21597>
24. Pavelyev, A.A. and Reshmin, A.I., Turbulent transition in the inlet region of a circular pipe, *Fluid Dyn.*, 2001, vol. 36, pp. 626–633.
<https://doi.org/10.1023/A:1012349915447>